The effect of using a high-albedo material on the Universal Temperature Climate Index within a street canyon

P.J.C. Schrijvers[a,c,*], H.J.J. Jonker[a,c], S.R de Roode[a,c], S. Kenjereš[b,c]

[a] *Atmospheric Physics Section, Department of Geoscience & Remote Sensing, Faculty of Civil Engineering and Geotechnology, Delft University of Technology, Stevinweg 1, 2628CN Delft, The Netherlands*

[b] *Transport Phenomena Section, Department of Chemical Engineering, Faculty of Applied Sciences, Delft University of Technology, Julianalaan 136, 2628BL, The Netherlands*

[c] *J.M. Burgers Centre for Fluid Dynamics, Julianalaan 136, 2628BL, The Netherlands*

Abstract

This study investigates the effect of different high-albedo adaptation strategies on air temperature, mean radiant temperature and the Universal Temperature Climate Index (UTCI) for a single idealized 2D street canyon. A simulation model has been used that computes these variables at 1 meter spatial resolution. Using high-albedo materials for all canyon surfaces decreases air temperature but increases mean radiant temperature, thereby increasing the UTCI. Differences in mean radiant temperature are much larger compared to differences in air temperature inside a single street canyon, and therefore have a larger impact on the UTCI. The impact of albedo-differences on the UTCI are relatively small compared to the large impact of shading. The best strategy for the outdoor environment with building height to width ratio H/W=0.5 was found to be a uniform albedo of 0.2. For H/W=1.0, an

*Corresponding author

Email address: `p.j.c.schrijvers@tudelft.nl` (P.J.C. Schrijvers)

albedo gradient from a high albedo at the bottom part and a low albedo at the top of the vertical walls showed the lowest UTCI. Air temperature increases slightly compared to a uniform albedo, but a large decrease in mean radiant temperature and the UTCI was found. Although using high-albedo material can mitigate the atmospheric urban heat island effect, it is very likely to increase pedestrian heat stress, which might not be the desired result.
Keywords: high-albedo material, urban heat island, adaptation measures, Universal Temperature Climate Index

1. Introduction

To counter the Urban Heat Island effect (UHI), the use of high-albedo materials is often advocated ([1, 2]). The general idea is that high-albedo materials reflect more solar radiation and thereby reduce the outdoor air temperature, which has been shown by many studies [3, 4, 5]. The effect of these high-albedo materials on air temperature is also studied by Taha et al. [6], where large scale albedo changes for ten regions in the USA are considered. A meso-scale model is used, wherein the urban environment is parametrized. The regions were characterized and simulated in reference- and modified-surface conditions. The simulations suggest that large-scale increases in albedo and vegetative fraction can result in spatially-averaged decreases in mid-day air temperature of -0.5K to -1.5K during a typical summer day. Peak reductions in air temperature are found of up to -5K locally.

Changing the albedo also impacts the indoor air temperature (or the cooling load of obstacles, which is more often studied [7, 8, 9]). The effect of using different albedo values on the indoor air temperature is studied (amongst others) by Givoni [10], in combination with the insulation thickness. Results show large temperature differences between indoor and outdoor when there is little insulation. The total effect on indoor air temperature when changing the albedo from black (α=0.18) to white (α=0.89) is -37K. With increasing insulation thickness, the temperature difference is reducing in magnitude. More energy is stored in the urban material and less energy is transferred that is able to heat indoor air.

Although a reduction in outdoor and indoor air temperature are considered positive effects, there are also adverse effects of using high-albedo materials, as shown by Erell et al. [5]. In this study the effect of high-albedo materials on the outdoor pedestrian heat stress is investigated for four cities by using the Canyon Air Temperature model (CAT, [11]). This model uses meteorological data from rural measurement locations to compute the local canyon air temperature, wind speed and radiative properties, and is used to compute the effect of different albedo values on the local thermal environment. The output of this model is then used to compute the Index of Thermal Strain (ITS model, [12]), which is a pedestrian stress parameter. It was found that using high-albedo material can lead to lower air temperatures, but to a higher value of the heat stress, due to the increase in reflected radiation that can reach the ground surface. The thermal stress is decreasing with increasing H/W ratio, independent of the albedo that is used. To quote the authors: *"The results of this study indicate that local benefits, in terms of pedestrian thermal comfort, are likely to be marginal at best and that high-albedo paving materials may actually increase thermal stress in warm environments."*

The current study, conducted as a part of the Dutch Climate Proof Cities consortium [13], aims to take the study by Erell et al. [5] one step further. Instead of using a parametrized model, a building resolving model is used which computes radiative transfer, heat conduction into the urban material and ventilation within the urban canyon at 1m spatial resolution. Furthermore, different test-cases are considered. Instead of using one albedo for all canyon surfaces, there is also differentiation between north-facing and south-facing walls and albedo gradients along the vertical walls. In this way the impact of using different albedo values on air temperature, mean radiant temperature and the Universal Temperature Climate Index (UTCI, [14]) can be studied. The model that is used is discussed in Section 2, as well as the UTCI and the different test cases considered. The results for different cases are discussed in Sections 3-7 (each section discusses a different adaptation strategy), after which conclusions are drawn in Section 8.

2. Methodology

2.1. The used model

The effect of different albedo adaptation measures is tested by using the building resolving model that was used in Schrijvers et al. [15, 16]. In this model, radiative transfer is computed by using a Monte-Carlo model, which computes absorbed radiation at the surface, the long-wave trapping effect and mean radiant temperature in detail. A Lambertian scatter function is used, indicating that the scattering angle at the surface is cosine-weighted. Mean radiant temperature is defined as the temperature that a human body would have if all absorbed radiation is emitted again through long wave radiation (the human body is in radiative equilibrium), and is computed by

$$T_{\mathrm{mrt}} = \sqrt[4]{\frac{S_{\mathrm{str}}}{\epsilon_{\mathrm{p}}\sigma}} \tag{1}$$

where S_{str} is the local mean radiant flux density, ϵ_{p} the emissivity of the human body (with a standard value of 0.97) and σ the Stefan-Boltzmann constant. The mean radiant flux density is the amount of both short wave and long wave radiation that is absorbed by a standing human body (and is an irradiance), and is computed by

$$S_{\mathrm{str}} = (1 - \alpha_{\mathrm{p}}) \sum_{i=1}^{6} K_i F_i + \epsilon_{\mathrm{p}} \sum_{i=1}^{6} L_i F_i \tag{2}$$

where α_{p} is the albedo of the human body (with a standard value of 0.3), K_i the total short wave radiative irradiance, L_i the total long wave radiative irradiance and F_i a geometric factor representing a standing human body. The index i is used for the six directions where radiation is entering from. The geometric factor F has a value of 0.22 for radiation entering from the west, east, south and north direction and 0.06 for radiation entering from the top and bottom, and represents a standing human body. Within the Monte-Carlo framework, computing the local mean radiant flux density is a matter of bookkeeping where the amount of radiative flux entering a grid cell is stored per direction and radiation type (either long wave or short wave). Since the current study is 2D, radiation entering from the east and west direction is taken equal to that of the averaged radiation entering from the north and south direction. This assumption can be seen as computing the mean radiant temperature for a large square that is surrounded by obstacles.

The transient 1D heat conduction equation is used to compute the energy transfer from a building or ground surface into the underlying urban material (conductive heat flux), while a Computational Fluid Dynamics (CFD) model is used to compute wind speed, air temperature and the sensible heat flux [15, 16, 17, 18, 19, 20].

The input-parameters of the model are shown in Table 1. The location considered is that of Amsterdam (the Netherlands) in the middle of June, the month where the sun reaches the highest elevation angle in the Netherlands. Free stream air temperature is 293.15K and constant with time. The same holds for the free stream wind speed of 4 ms^{-1}. The model uses an initial guess of surface temperature, that is used to compute the air temperature and heat fluxes at the first time step. Ten days are simulated to ensure that the chosen initial conditions do not impact the final results. A time step of 6 minutes is used, where surface temperature is fed back to all sub-models in this time-instance.

The model is extended with the computation of the UTCI. This is an apparent temperature, which takes into account air temperature, wind speed, radiation, humidity, metabolism of the human body and clothing insulation worn by the subject. The UTCI is defined as the isothermal air temperature of the reference condition that would elicit the same dynamic response (strain) of the physiological model [21].

As the dynamic response of the UTCI-model is multidimensional (due to changes in the body core temperature, sweat rate, skin wettedness, etc.) this would require long computation times. To overcome this problem, a fortran90 sub-routine is available from the UTCI-website (www.utci.org/utcidoku.php), where a sixth order polynomial function is available to compute the UTCI. This function uses air temperature, mean radiant temperature, wind speed and relative humidity as input, and the energy balance between human core and skin, and between skin and clothing is parametrized. The range where this polynomial fit is valid ranges from:

- $223\text{K} \leq T_{\text{a}} \leq 323\text{K}$
- $-30\text{K} \leq T_{\text{mrt}} - T_{\text{a}} \leq +70\text{K}$
- $0.5\text{ms}^{-1} \leq u_{10\text{m}} \leq 17\text{ms}^{-1}$

Since the local UTCI inside the canyon is studied here, the wind speed at each grid cell inside the street canyon is used instead of the wind speed at 10m height. In this way, changes in wind speed due to the different adaptation measures are taken into account. Relative humidity is not computed in the current model, and is therefore set to a fixed value of 50% throughout the canyon.

The UTCI uses an assessment scale, which is shown in Table 2. This relates the UTCI temperature to the amount of heat stress that a human would undergo. It must be noted that all temperatures throughout this manuscript are in Kelvin, except the UTCI, which is defined as the temperature in °C. The range extends to negative temperatures (cold stress), but since this is not considered in this study, this is not shown here.

The UTCI is designed to be applicable in all climates, seasons, and time and spatial scales. The advantage of using the UTCI is that all effects of an adaptation measure on the outdoor environment are captured in one number, that is directly related to the amount of heat stress.

2.2. Adaptation measures

Different adaptation measures are tested for an idealized 2D geometry with square obstacles which are equal in height and spaced equally. The building width (B) is 25m, distance between the obstacles (W) is 50m, while building height is varied between H=25m (H/W=0.5) and H=50m (H/W=1.0). The 2D geometry bounds the model to cases where ventilation is mainly a 2D effect. For higher obstacles, it was found that 3D effects become more important [15], and are therefore not used in this study. A north-south facing canyon is considered, where the south facing wall is sunlit throughout the day.

As a first test, the albedo (α) of all canyon surfaces is varied from 0.2 (case 1), 0.4 (case 2) and 0.6 (case 3) respectively. These values for the albedo are also used for studying other adaptation strategies in this study. An albedo of 0.2 corresponds to weathered asphalt, 0.4 to concrete and 0.6 to 'white-washed' surfaces. These values are on the edges of realizable and are used to identify the maximum effect of the adaptation measures.

The impact of long wave effects is also quantified for different values of the emissivity ϵ, where ϵ is modified from 0.95 (case 2), 0.90 (case 4) and 0.85 (case 5). One could hypothesise that decreasing the emissivity could lead to a positive feedback effect (less absorbed radiation from the sky, lower surface temperature, less long wave trapping, lower surface temperature, etc.), which could have a significant effect on the UTCI. Other test cases are shown in Fig. 1. Case 6 and case 7 investigate the effect of differentiating the albedo of the north and south wall, by using an albedo of 0.6 on one vertical surface and an albedo of 0.2 on the other surface. The effect of using a vertical

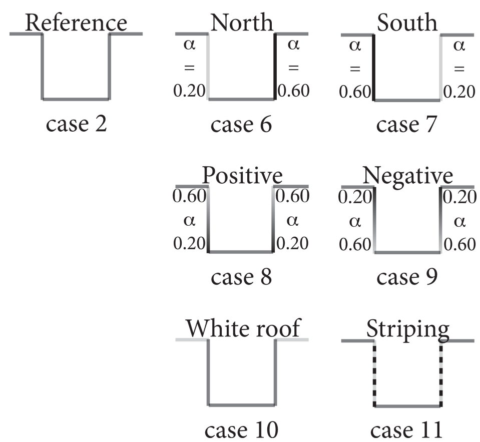

Figure 1: Graphic representation of different albedo adaptation strategies. Cases with uniform albedo (cases 1, 2 and 3) or uniform emissivity (cases 2, 4 and 5) are not shown here. Note that the solar position is always on the left side of the canyon.

albedo gradient is studied for cases 8 and 9, where a positive gradient (from a low-albedo bottom part to a high-albedo top part of the vertical wall) and a negative gradient (reversed) are used, respectively. Case 10 investigates the effect of a white roof (α=0.6 on all roof surfaces instead of the reference value of α=0.4). The hypothesis is that this reduces the ambient air temperature entering the canyon, which could have a reducing effect on the UTCI. Case 11 investigates the impact of striping, where strips with different albedo values of 0.6 and 0.2 are used on the vertical walls. The reasoning is that this creates large spatial differences in surface temperature and therefore invigorates convection.

3. Uniform albedo effect

3.1. Diurnal cycle

The first question addressed is how different albedo values affect the daily cycle of surface temperature inside the canyon. Therefore, time series of surface temperature are shown in Fig. 2. One point in the centre of the street canyon is shown here for H/W=0.5, and displays a large variation in temperature, ranging from 290K during the night to 315K during day (for the α=0.2 case). Large effects of changing albedo can be found during the day when the point is directly sunlit, with surface temperature differences of 5K between the cases. However, the effect during periods when the measurement point is in the shade (morning, afternoon) are small. This is also the case during the night, where the surface temperature is mainly controlled by long wave radiation. The conductive heat flux does show differences for the cases during night (not shown here), and is reducing (closer to zero) with increasing albedo (lighter canyon). For the high-albedo case, less energy is transferred into the material during the day, and therefore also less energy released during the night.

Since variations during the night are small, this study will only consider the effect at mid-day of the last diurnal cycle.

3.2. Distributions within a street canyon

Spatial changes as a result of different albedo values are shown in Fig. 3 for surface temperature (top panel), air temperature at 2m height (middle panel) and mean radiant temperature at 2m (bottom panel). Solid lines are used for H/W=0.5, while dash-dotted lines are used for H/W=1.0. Surface

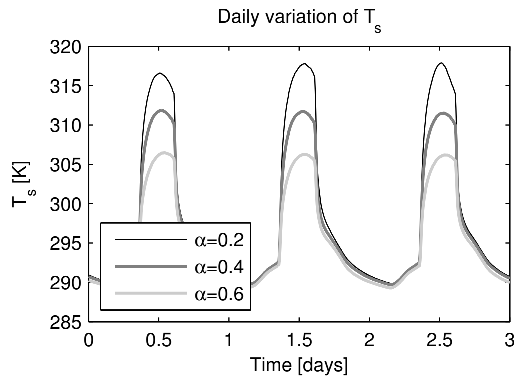

Figure 2: Daily variation in surface temperature for one point in the centre of the street canyon (H/W=0.5) for three different albedo values.

temperatures are plotted according to the inset in the top panel, where all vertical surfaces are scaled to uniform height, to allow comparison of different H/W ratios. Results for air temperature, mean radiant temperature and the UTCI are also summarized in Table 3. A low albedo increases surface temperature by as much as +5K (H/W=0.5) and +14K (H/W=1.0) at the ground level compared to the reference case, while the effect is negligible in the shaded areas. The high-albedo case changes surface temperature by −5K (H/W=0.5) and −8K (H/W=1.0) in the sunlit areas. The effect of changing the albedo on surface temperature becomes smaller towards roof levels.

The change in surface temperature impacts air temperature directly (middle panel of Fig. 3), which is lower for the high-albedo case. For H/W=0.5, the difference in air temperature is (canyon averaged) +0.2K for α=0.2 and −0.4K for α=0.6 compared to the reference case (α=0.4). Note that the absolute air temperature is lower for H/W=1.0 compared to H/W=0.5.

In addition to air temperature profiles, patterns of air temperature and

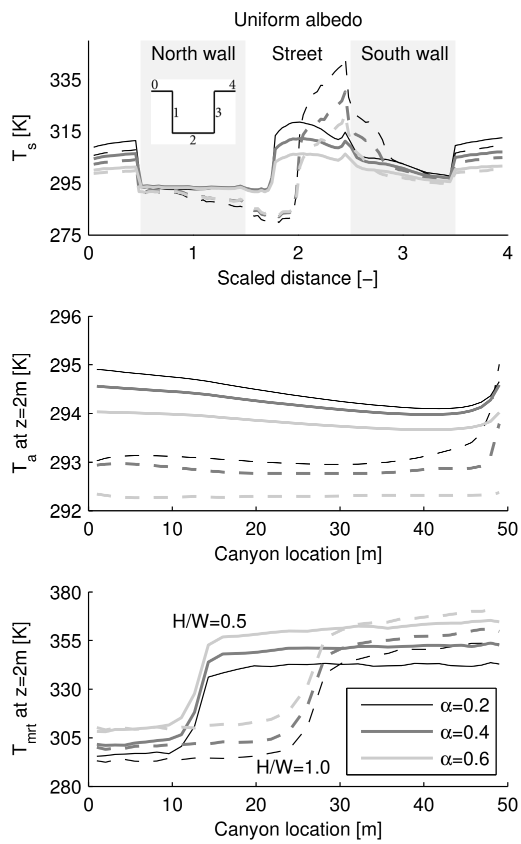

Figure 3: Effect of albedo changes on surface temperature (top panel), air temperature at 2m height (middle panel) and mean radiant temperature at 2m height (bottom panel). Gray scales are used for different cases, as indicated in the legend in the bottom panel. Solid lines are used for H/W=0.5, while dash-dotted lines are used for H/W=1.0. Air temperature and mean radiant temperature are displayed as a function of canyon position.

wind speed are shown in Fig. 4 for H/W=0.5 (left) and H/W=1.0 (right) and the three different cases considered (vertical plots). This again shows that a low albedo creates a warmer canyon, where there is a larger sensible heat flux due to the increased absorbed short wave radiation. For H/W=0.5, there is one recirculating vortex for all cases, where the strength is independent of the albedo. For H/W=1.0, there are two counter rotating vortices, where the warm south-facing wall creates buoyancy forces that are large enough to create a second vortex that spans the bottom part of the canyon. The strength of this vortex is dependent on the albedo, where a low albedo (higher surface temperature) creates a stronger vortex. The air temperature profile at 2m height shows relatively modest changes in air temperature compared to the remainder of the canyon.

Mean radiant temperature (bottom panel Fig. 3) is impacted by the change in reflected short wave radiation, but also by the the change in emitted long wave radiation by the walls due to changing surface temperature. The contrary effect to air temperature is shown for T_{mrt}, where the high-albedo case shows a higher mean radiant temperature (+9.5K for H/W=0.5). However, changes in mean radiant temperature due to changing values of the albedo are modest when compared to the effect of shading, where T_{mrt} is over -40K lower in the shaded areas compared to the sunlit areas. For H/W=1.0, there is a larger area in the shade, with substantially lower T_{mrt} as a consequence. In the sunlit part of the canyon, T_{mrt} is higher for H/W=1.0 compared to H/W=0.5 due to increased multiple reflections of short wave radiation. T_{mrt} is controlled by the large contributions of direct short wave radiation (which has a maximum value of 900 Wm^{-2} in the sunlit area) and

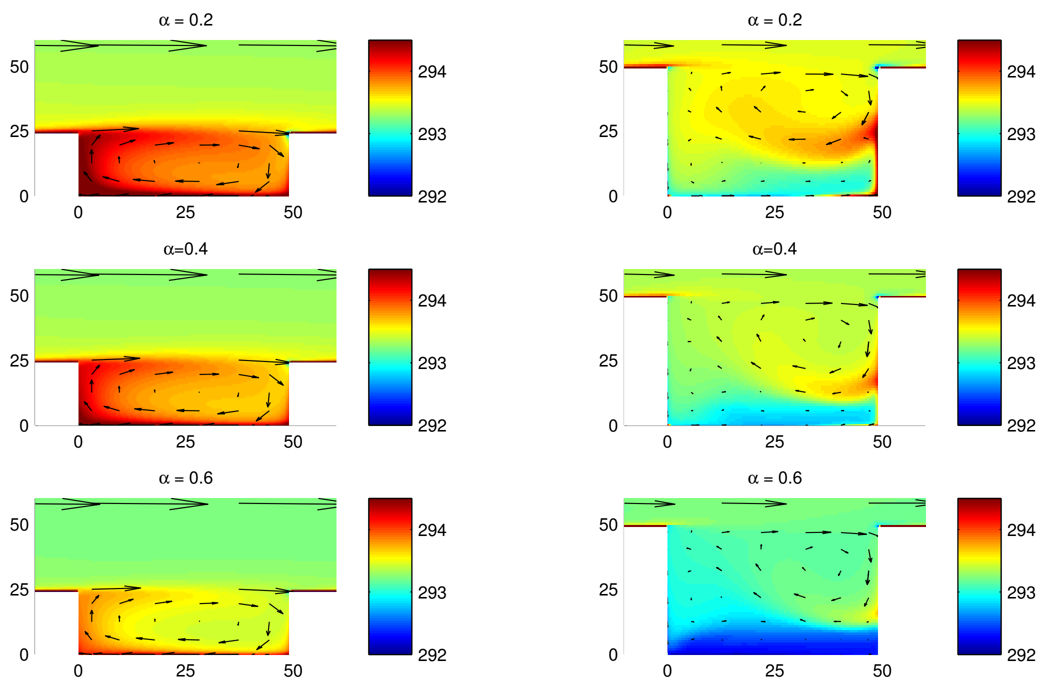

Figure 4: Spatial overview of air temperature for H/W=0.5 (left panels) and H/W=1.0 (right panels) when albedo is changed uniformly over the entire canyon. The same colour axis is used for all sub plots. Local wind is indicated by arrows, where the top arrows at H/W=0.5 show a wind speed of $4 \mathrm{ms}^{-1}$.

the long wave trapping effect (with a maximum contribution of 700 Wm^{-2}). This results in a T_{mrt} of 350K (sunlit part, H/W=0.5, α=0.4). When this values are compared to measurements of mean radiant temperature in the city of Goteborg, Sweden [23], the values obtained in this study are higher then obtained from measurements, where a maximum T_{mrt} was found of 340K for a large open square with α=0.4. This is partly due to the 2D assumption where radiative fluxes from the east and west direction are taken equal to the average of the north and south direction. Next to this 2D assumption, this study considers highly idealized conditions, where there is no vegetation, no latent heat flux and clear blue skies, thereby allowing for these large radiative fluxes.

Values of air temperature and mean radiant temperature are combined in the computation of the UTCI. This shows an increase for high-albedo canyons (see Fig. 5), by as much as +2°C for both H/W ratios compared to the reference case. Using a low albedo changes the UTCI by −1.9°C for both H/W ratios. The effect of changing the albedo however is small compared to the shading effect, which changes the UTCI by as much as −12°C, thereby indicating only 'moderate heat stress' if there is any stress at all. This is mainly due to the large decrease of direct short wave radiation, which impacts mean radiant temperature and therefore UTCI. The local change in air temperature only has a small effect. To compensate an increase in T_{mrt} of +15K, air temperature should change by −7K to maintain the same UTCI temperature for this case.

Erell et al. [5] concluded that the thermal stress is decreasing with increasing H/W ratio, independent of the albedo value. This study shows that

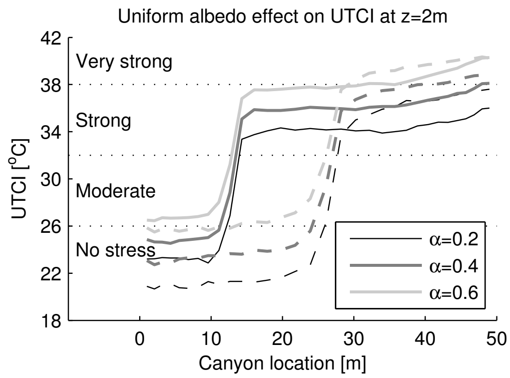

Figure 5: The UTCI temperature for different values of the albedo, where albedo is changed over the entire canyon. Solid lines indicate H/W=0.5, dash-dotted lines are used for H/W=1.0.

this does not hold for all locations in the canyon, where for H/W=1.0 the UTCI is lower in the shaded part compared to H/W=0.5, but higher in the sunlit part due to increased multiple reflections.

4. Uniform emissivity effect

In addition to changing the canyon albedo, the effect of changing the emissivity is tested. The effect of these changes on the UTCI are shown in Fig. 6 and in Table 4 for the different cases, and show modest effects. A decrease in the emissivity from 0.95 to 0.85 did not change the UTCI for H/W=0.5 and increased the UTCI by +0.4°C for H/W=1.0.

The amount of radiation that is absorbed at the surface is slightly decreasing with decreasing emissivity. However, this effect is much lower compared to the albedo case. This is due to the high value of the emissivity, where the amount of energy involved with multiple reflections is much smaller compared to the albedo cases. Next to this, the physical range that can be

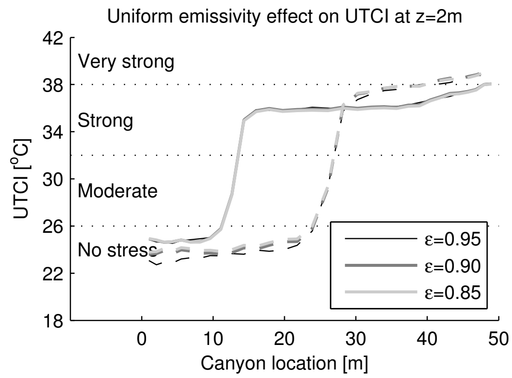

Figure 6: The UTCI temperature for different values of the emissivity, where emissivity is changed over the entire canyon. Solid lines indicate H/W=0.5, dash-dotted lines are used for H/W=1.0.

occupied by the emissivity is much smaller. Since the change in surface temperature is small, there is also a small effect on the long wave trapping effect. For H/W=0.5, the positive feedback effect is present, but is very weak. For H/W=1.0, there is even a negative feedback, for which the air temperature is increasing faster then the mean radiant temperature is decreasing.

5. Differentiating albedo of the street canyon vertical walls

In this section, case 6 (with a high-albedo for the north-facing wall) and case 7 (high-albedo for the south-facing wall) are compared to the reference case 2 with a uniform albedo (see Fig. 1 for a graphic representation).

Varying the albedo of vertical walls has an impact on surface temperature, as shown in the top panel of Fig. 7, where surface temperature changed for case 7 at the lower corner between south wall and ground by −8K (−12K) for H/W=0.5 (H/W=1.0), while the north wall is heated by +2K compared to the reference case for both H/W ratios. Heating of the north wall is due to the increased energy involved with multiple reflections originating from the south wall in combination with the lower albedo at the north wall. The impact of case 6 is however much smaller, with 'only' a reduction in surface temperature of -1.5K (-3.0K) for H/W=0.5 (H/W=1.0) at the north wall, while the surface temperature of the low-albedo south wall is increasing by +7K (+15K) for H/W=0.5 (H/W=1.0). Although the north wall has a higher albedo in this case, all short wave radiation absorbed at the north wall is either diffuse from the sky or reflected from an other surface, from which the radiative flux is much lower.

Air temperature profiles show a significant change of up to +0.7K for case 7 (results are also summarized in Table 5). However, the most interesting phenomena can only be seen from the spatial air temperature patterns, as shown in Fig 9. For H/W=0.5, this shows that case 7 is much colder compared to the reference case due to the lower surface temperature at the south wall. For H/W=1.0, case 7 results in a higher air temperature at the bottom of the canyon. This results from a change in vortex dynamics between the different cases. For the reference case and case 6 there are two counter rotating vortices, where cold air is trapped at the lower part of the canyon. For case 7, the surface temperature at the south wall is lower, there is less warm air rising and the forced convection (due to the free stream air flow) dominates over natural convection (due to buoyancy forces). This results in one single vortex which spans the whole canyon. Due to the change in vortex dynamics, the considered adaptation measures show different effect on air temperature for different H/W ratios. This stresses the importance of CFD modelling, where a change in albedo can have large impacts on air flow patterns. This does not only impact air temperature, but can also impact pollutant dispersion.

As a result of different albedo values, the mean radiant temperature is also affected (bottom panel of Fig. 7), where case 6 (low-albedo south wall) decreases mean radiant temperature by more than -2K for case 7.

Despite the changes in surface temperature, air temperature and mean radiant temperature, the effect of differentiation the albedo of the north and south wall on the UTCI is small for H/W=0.5 (see Fig. 8). Both cases reduce the UTCI by -0.2°C for H/W=0.5

For H/W=1.0, larger differences are present, where case 6 reduces the UTCI by -1.1°C, while case 7 with the high-albedo south wall increases the UTCI by $+0.3$°C. Both cases indicate that a low-albedo south wall reduces the UTCI, despite the increase in air temperature, again indicating the large impact of short wave radiation.

6. Vertical albedo gradients

Instead of changing the albedo of the entire wall, two case are conducted where there is an albedo gradient on the vertical walls (case 8, which uses a high-albedo at the top, and case 9 which uses a low albedo at the top, see Fig. 1).

Changes in surface temperature due to the changed albedo are mainly present at the bottom part of the south wall (Fig. 10), with maximum changes of $+7$K for case 8 and -7K for case 9.

Despite the modest changes in surface temperature, the results on air temperature are significant (see Table 6), with a decrease of -0.4K (H/W=0.5)

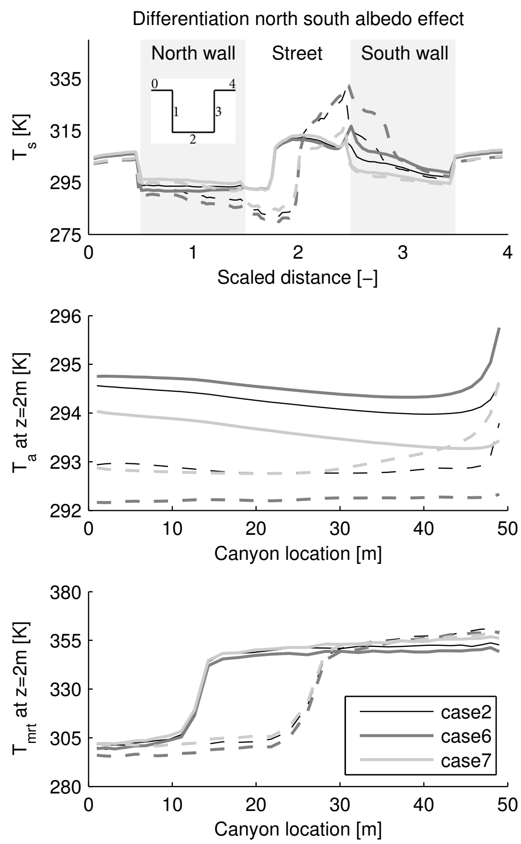

Figure 7: Effect of differentiating albedo of north and south wall on surface temperature (top panel), air temperature at 2m height (middle panel) and mean radiant temperature at 2m height (bottom panel). Cases are shown in Fig. 1.

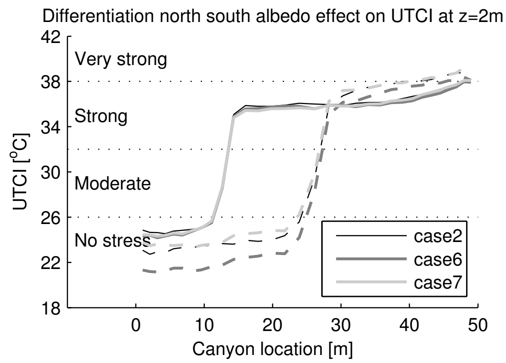

Figure 8: Effect of differentiating albedo of north and south wall on the UTCI, compared to the reference case with an uniform albedo of 0.4.

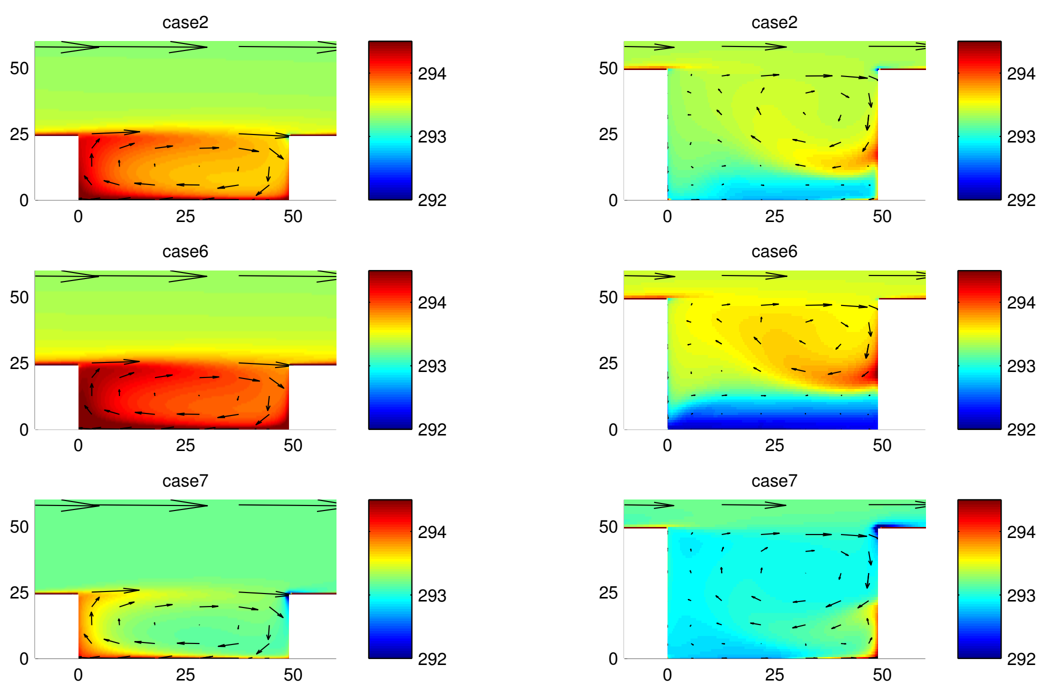

Figure 9: Spatial overview of air temperature for H/W=0.5 (left panels) and H/W=1.0 (right panels) for reference cases (top), case 6 (high-albedo north wall, middle) and case 7 (high-albedo south wall, bottom).

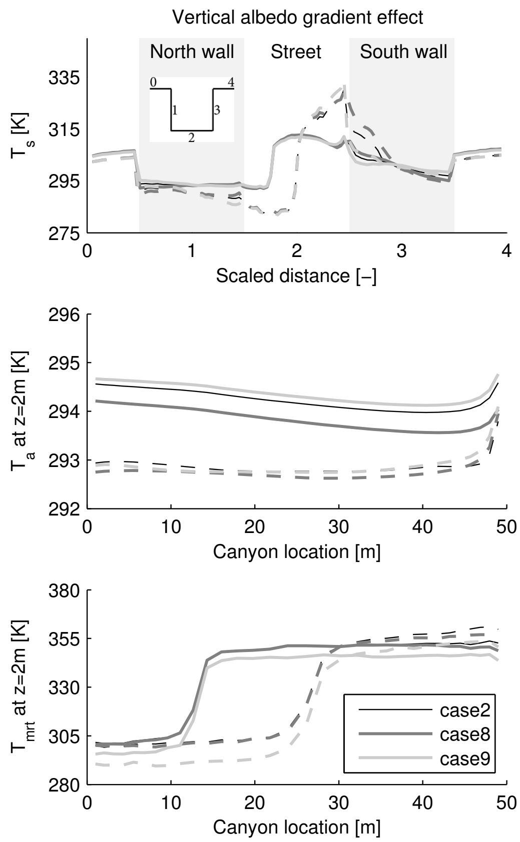

Figure 10: Effect of vertical albedo gradients on surface temperature (top panel), air temperature at 2m height (middle panel) and mean radiant temperature at 2m height (bottom panel).

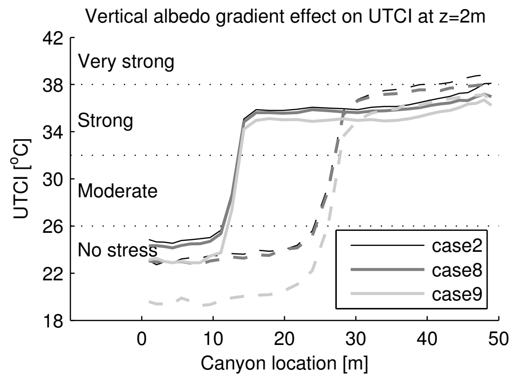

Figure 11: Effect of vertical albedo gradients on the UTCI, compared to the reference case with an uniform albedo of 0.4. Case 8 uses a high albedo at the top part of the vertical wall, case 9 a low albedo.

for case 8 and an increase of +0.8K for case 9. With a high albedo at the upper part of the canyon, there is less heating of ambient air at the top of the canyon, which has a lasting impact on the remainder of the canyon. The recirculating air is heating inside the canyon, but due to the lower initial temperature, the canyon as a whole remains colder.

The mean radiant temperature is decreasing for both cases compared to the reference case. For case 9, mean radiant temperature decreases by −7.4K and −8.6K for H/W=0.5 and H/W=1.0 respectively. For case 8, this is −0.7K and −1.2K. For case 9 (low-albedo top part), more short wave radiation is absorbed at the top of the canyon, and less radiation is reflected towards the ground surface. This effect is present for both direct short wave and diffuse short wave radiation. For case 8, the high-albedo top of the canyon reflects more radiation into the canyon, which is absorbed at the lower parts of the vertical walls.

If all effects are combined into the UTCI, a decrease is shown for both cases. Case 8 case shows a decrease of -0.4°C for both H/W ratios, while case 9 decreases the UTCI by-1.1°C for H/W=0.5 and -2.7°C for H/W=1.0. This decrease in the UTCI is larger for case 9 than a uniform albedo of 0.2 and is thereby the most efficient measure to reduce the outdoor thermal comfort for H/W=1.0 in this study.

7. White roof and striping

Results for the UTCI for cases 10 and 11 are shown in Fig. 12 and Table 7 and display small changes in the UTCI compared to the reference case. For case 10 (white roof), there is indeed a reduction in ambient air temperature as hypothesised for H/W=1.0, but this is modest (-0.1K). This reduction is not present for H/W=0.5. Mean radiant temperature is also impacted, which leads to an increase in the UTCI of $+0.2^{\circ}$C for H/W=0.5.

Case 11 (striping) has a large impact on surface temperature, where local differences of up to 10K are found compared to the reference case. However, these temperature differences are diffused rapidly when air temperature is considered, and show an increase for H/W=0.5 (+0.8K) but a decrease for H/W=1.0 (-0.6K). Mean radiant temperature shows opposite effects to air temperature. This results in a small impact on the UTCI for H/W=0.5 ($+0.3^{\circ}$C) and a decrease in the UTCI for H/W=1.0 of (-0.3°C).

8. Conclusions

This systematic study investigated the effect of different albedo adaptation strategies for an idealized 2D street canyon. Using high-albedo materials for all canyon surfaces decreases air temperature but increases mean radiant

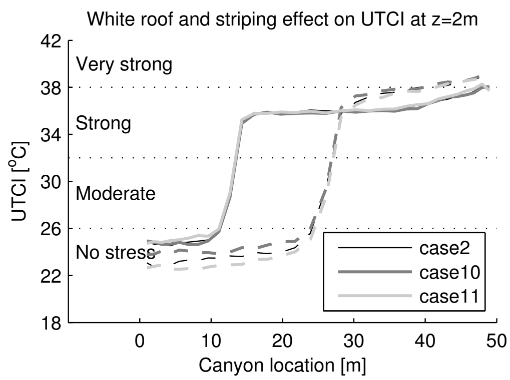

Figure 12: Effect of white roof (case 10) and striping (case 11) on the UTCI, compared to the reference case with an uniform albedo of 0.4.

temperature, leading to an increase in the UTCI (more heat stress). If only the UTCI is considered, a higher albedo increases heat stress, consistent with [5].

Differentiating the albedo of the north and south wall shows similar findings. A low-albedo south wall increases air temperature but lowers mean radiant temperature, with a decrease in the UTCI as a consequence. This different behaviour of air temperature and mean radiant temperature is observed for all cases.

The best strategy (with the simplified test cases considered) was found to be a vertical gradient of albedo for H/W=1.0, with a high albedo at the bottom part and low albedo at the top part of the wall. Air temperature increases slightly compared to a uniform albedo of α=0.4, but reduces the UTCI the most (-2.7 °C). For H/W=0.5, a uniform low albedo resulted in the lowest heat stress (-1.9 °C) where the increase in air temperature is compensated by a large decrease in mean radiant temperature.

The maximum effect that is achieved by using different albedo values is around -2°C on the UTCI. However, the UTCI is reduced by up to -12°C in shaded areas compared to the sunlit areas. This shadow-effect is also seen for the different H/W ratio: for every case investigated, the canyon-average UTCI-value is lower for H/W=1.0 compared to H/W=0.5, although local values of the UTCI for H/W=1.0 can exceed that of H/W=0.5. Therefore, it might be worthwhile to investigate artificial shading measures, which can be closed during day (reduce short wave radiation) and opened during night (increase ventilation and reduce long wave trapping).

This study also showed that changing albedo values can alter the vortex dynamics inside a street canyon. Although the effect on air temperature is modest, this can have large consequences on pollutant dispersion. Exhaust gasses of cars can be trapped in the bottom part of the canyon, or more easily dispersed throughout the canyon, dependent on the flow dynamics.

It must be noted that only the outdoor situation is considered in this study, and that the effect on the indoor environment can show opposite effects. Furthermore, the cases considered are highly idealized and only consider a 2D geometry. However, this study does indicate that there are adverse effects of using high-albedo materials, where air temperature and mean radiant temperature often show opposite effects. This indicates that simply using high-albedo material wherever possible might not lead to the desired results.

9. Acknowledgment

We would like to thank Victor Vertregt and Franka Veltman with their help in developing the Monte-Carlo radiation model and implementation of the mean radiant temperature. This study is funded by the Dutch Climate Proof Cities consortium, which is part of the Knowledge for Climate program (http://knowledgeforclimate.climateresearchnetherlands .nl/climateproofcities).

References

[1] H. Akbari, M. Pomerantz, H. Taha, Cool surfaces and shade trees to reduce energy use and improve air quality in urban areas, Solar Energy 70 (2001) 295 – 310. Urban Environment.

[2] A. Synnefa, A. Dandou, M. Santamouris, M. Tombrou, N. Soulakellis, On the use of cool materials as a heat island mitigation strategy, Journal of Applied Meteorology and Climatology 47 (2008) 2846–2856.

[3] H. R. Silva, R. Bhardwaj, P. E. Phelan, J. S. Golden, S. Grossman-Clarke, Development of a zero-dimensional mesoscale thermal model for urban climate, Journal of Applied Meteorology and Climatology 48 (2009) 567–668.

[4] M. Santamouris, N. Gaitani, A. Spanou, M. Saliari, K. Giannopoulou, K. Vasilakopoulou, T. Kardomateas, Using cool paving materials to improve microclimate of urban areas design realization and results of the flisvos project, Building and Environment 53 (2012) 128 – 136.

[5] E. Erell, D. Pearlmutter, D. Boneh, P. B. Kutiel, Effect of high-albedo materials on pedestrian heat stress in urban street canyons, Urban Climate (2013). In press.

[6] H. Taha, S. Konopacki, S. Gabersek, Impacts of large-scale surface modifications on meteorological conditions and energy use: A 10-region modeling study, Theoretical and Applied Climatology 62 (1999) 175–185.

[7] H. Taha, H. Akbari, A. Rosenfeld, J. Huang, Residential cooling loads and the urban heat islandthe effects of albedo, Building and Environment 23 (1988) 271 – 283.

[8] J. Simpson, E. McPherson, The effects of roof albedo modification on cooling loads of scale model residences in tucson, arizona, Energy and Buildings 25 (1997) 127 – 137.

[9] S. Bretz, H. Akbari, A. Rosenfeld, Practical issues for using solar-reflective materials to mitigate urban heat islands, Atmospheric Environment 32 (1998) 95 – 101. Conference on the Benefits of the Urban Forest.

[10] B. Givoni, Man, Climate and Architecture, Applied Science, London, 1976.

[11] E. Erell, T. Williamson, Simulating air temperature in an urban street canyon in all weather conditions using measured data at a reference meteorological station, International Journal of Climatology 26 (2006) 1671–1694.

[12] D. Pearlmutter, P. Berliner, E. Shaviv, Integrated modeling of pedestrian energy exchange and thermal comfort in urban street canyons, Building and Environment 42 (2007) 2396 – 2409.

[13] R. A. W. Albers, P. Bosch, B. Blocken, A. V. D. Dobbelsteen, L. V. Hove, T. Spit, Overview of challenges and achievements in the Climate Proof Cities program, Building and Environment (2014). In Press.

[14] D. Fiala, G. Havenith, P. Bröde, B. Kampmann, G. Jendritzky, UTCI-Fiala multi-node model of human heat transfer and temperature regulation, International Journal of Biometeorology 56 (2012) 429–441.

[15] P. J. C. Schrijvers, H. J. J. Jonker, S. Kenjeres, S. R. de Roode, Breakdown of the night time urban heat island energy budget, Building and Environment (2014). In press.

[16] P. J. C. Schrijvers, H. J. J. Jonker, S. Kenjeres, S. R. de Roode, On the local day time urban heat island of an idealized 2D city, Journal of Applied Meteorology and Climatology (2014). Manuscript submitted for publication.

[17] S. Kenjeres, K. Hanjalic, Transient analysis of Rayleigh-Benard convection with a RANS model, International Journal of Heat and Fluid Flow 20 (1999) 329 – 340.

[18] S. Kenjeres, K. Hanjalic, LES, T-RANS and hybrid simulations of thermal convection at high Ra numbers, International Journal of Heat and Fluid Flow 27 (2006) 800 – 810.

[19] S. Kenjeres, K. Hanjalic, Tackling complex turbulent flows with transient RANS, Fluid Dynamics Research 41 (2009) 012201.

[20] S. Kenjeres, B. ter Kuile, Modelling and simulations of turbulent flows in

urban areas with vegetation, Journal of Wind Engineering and Industrial Aerodynamics 123, Part A (2013) 43 – 55.

[21] G. Jendritzky, R. de Dear, G. Havenith, UTCI Why another thermal index?, International Journal of Biometeorology 56 (2012) 421–428.

[22] P. Bröde, D. Fiala, K. Bazejczyk, I. Holmer, G. Jendritzky, B. Kampmann, B. Tinz, G. Havenith, Deriving the operational procedure for the Universal Thermal Climate Index (UTCI), International Journal of Biometeorology 56 (2012) 481–494.

[23] F. Lindberg, B. Holmer, S. Thorsson, SOLWEIG 1.0 Modelling spatial variations of 3D radiant fluxes and mean radiant temperature in complex urban settings, International Journal of Biometeorology 52 (2008) 697–713.

	Radiation
Latitude	52° 22' N
Longitude	4° 53' E
Start day	2012-06-10 00:00
End day	2012-06-20 23:59
max SW_{dir}	833.1 Wm^{-2}
max SW_{dif}	84.2 Wm^{-2}
	Heat conduction
λ	0.72 $\mathrm{Wm}^{-1}\mathrm{K}^{-1}$
ρ	1920 kgm^{-3}
C_{v}	835 $\mathrm{Jkg}^{-1}\mathrm{K}^{-1}$
Δwall	0.25m
Δground	1.00m
	CFD
T_{a}	293.15 K
U	4.0 m/s
cell width	1.0 m
cell expansion	5 %
max cell size	25 m

Table 1: Input constants for radiation, heat conduction into the urban material and the CFD model.

UTCI [°C]	Stress category
$> +46$	Extreme heat stress
+38 to +46	Very strong heat stress
+32 to +38	Strong heat stress
+26 to +32	Moderate heat stress
+9 to +26	No thermal stress

Table 2: Assesment scale of the Universal Temperature Climate Index [22].

	T_a [K]	T_{mrt} [K]	UTCI [°C]
α=0.2	+0.2 / +0.3	-8.1 / -7.3	-1.9 / -1.9
α=0.6	-0.4 / -0.6	+9.5 / +9.7	+2.0 / +2.1

Table 3: Effect of uniform albedo changes on air temperature, mean radiant temperature compared to reference case of α=0.4. Values indicate results for H/W=0.5 and H/W=1.0 (left and right respectively).

	T_a [K]	T_{mrt} [K]	UTCI [°C]
ϵ=0.90	0.0 / +0.2	0.0 / 0.0	0.0 / +0.3
ϵ=0.85	0.0 / +0.5	0.0 / -0.1	0.0 / +0.4

Table 4: Effect of uniform emissivity changes on air temperature, mean radiant temperature compared to reference case of ϵ=0.95. Values indicate results for H/W=0.5 and H/W=1.0 respectively.

	T_a [K]	T_{mrt} [K]	UTCI [°C]
case 6	+0.3 / -0.7	-2.2 / -2.7	-0.2 / -1.1
case 7	-0.6 / +0.2	+1.7 / +0.2	-0.2 / +0.3

Table 5: Effect of differentiation albedo values of vertical walls on air temperature, mean radiant temperature compared to reference case of α=0.4. Values indicate results for H/W=0.5 and H/W=1.0 respectively. Case 6 uses a low albedo on the south-facing wall, while case 7 uses a high albedo.

	T_a [K]	T_{mrt} [K]	UTCI [°C]
Case 8	-0.4 / -0.1	-0.7 / -1.2	-0.4 / -0.4
Case 9	+0.8 / 0.0	-7.4 / -8.6	-1.1 / -2.7

Table 6: Effect of albedo gradients on air temperature, mean radiant temperature compared to reference case of α=0.4. Case 8 uses a high albedo at the top part of the vertical wall and low albedo at the bottom part, case 9 the reversed. Values indicate results for H/W=0.5 and H/W=1.0 respectively.

	T_a [K]	T_{mrt} [K]	UTCI [°C]
Case 10	+0.1 / -0.1	+0.4 / +0.2	+0.2 / +0.1
Case 11	+0.8 / -0.6	-1.7 / -0.7	+0.3 / -0.3

Table 7: Effect of white roofs (case 10) and striping (case 11) on air temperature, mean radiant temperature compared to reference case of α=0.4. Values indicate results for H/W=0.5 and H/W=1.0 respectively.